CHEMISTRY
A EUROPEAN JOURNAL

FULL PAPER

DOI: 10.1002/chem.201300889

Identification of the Structural Determinants for Anticancer Activity of a Ruthenium Arene Peptide Conjugate

Samuel M. Meier,[a, b] Maria Novak,[a] Wolfgang Kandioller,[a, b] Michael A. Jakupec,[a, b] Vladimir B. Arion,[a] Nils Metzler-Nolte,[c] Bernhard K. Keppler,[a, b] and Christian G. Hartinger*[a, b, d]

Abstract: Organometallic Ru(arene)–peptide bioconjugates with potent in vitro anticancer activity are rare. We have prepared a conjugate of a Ru(arene) complex with the neuropeptide [Leu^5]-enkephalin. [Chlorido(η^6-*p*-cymene)(5-oxo-κO-2-{(4-[(*N*-tyrosinyl-glycinyl-glycinyl-phenylalanyl-leucinyl-NH_2)propanamido]-1*H*-1,2,3-triazol-1-yl)methyl}-4*H*-pyronato-κO)ruthenium(II)] (**8**) shows antiproliferative activity in human ovarian carcinoma cells with an IC_{50} value as low as 13 μM, whereas the peptide or the Ru moiety alone are hardly cytotoxic. The conjugation strategy for linking the Ru(cym) (cym = η^6-*p*-cymene) moiety to the peptide involved N-terminal modification of an alkyne-[Leu^5]-enkephalin with a 2-(azidomethyl)-5-hydroxy-4*H*-pyran-4-one linker, using Cu^I-catalyzed alkyne–azide cycloaddition (CuAAC), and subsequent metallation with the Ru(cym) moiety. The ruthenium-bioconjugate was characterized by high resolution top-down electrospray ionization mass spectrometry (ESI-MS) with regard to peptide sequence, linker modification and metallation site. Notably, complete sequence coverage was obtained and the Ru(cym) moiety was confirmed to be coordinated to the pyronato linker. The ruthenium-bioconjugate was analyzed with respect to cytotoxicity-determining constituents, and through the bioconjugate models [{2-(azidomethyl)-5-oxo-κO-4*H*-pyronato-κO}chloride (η^6-*p*-cymene)ruthenium(II)] (**5**) and [chlorido(η^6-*p*-cymene){5-oxo-κO-2-([(4-(phenoxymethyl)-1*H*-1,2,3-triazol-1-yl]methyl)-4*H*-pyronato-κO}ruthenium(II)] (**6**) the Ru(cym) fragment with a triazole-carrying pyronato ligand was identified as the minimal unit required to achieve in vitro anticancer activity.

Keywords: antitumor agents · bioorganometallic chemistry · mass spectrometry · peptide bioconjugates · ruthenium complexes

Introduction

Peptides are useful carriers for the specific accumulation of drugs in desired tissues and/or cell compartments.[1–5] In diagnostic and therapeutic metallodrug research,[6] the approach of tagging metal fragments to peptides is an emerging targeting strategy and several recent investigations were dedicated to organometal–peptide conjugation.[7–17] The peptide carrier is typically obtained by solid phase synthesis, and the metallodrug is linked to the peptide either on solid support or in solution after peptide cleavage from the resin. The metal can be conjugated directly via a suitable amino acid, or a linker with metal-chelating properties can be incorporated into the peptide sequence.[14,18] When pursuing the latter strategy, N-terminal and intrasequence derivatizations are most commonly used for metal-tagging. Moreover, most of the reported metal–peptide bioconjugates are synthesized with inert linkers.[14] Based on these strategies, encouraging but rare examples of anticancer active metal–peptide bioconjugates were reported with different metal systems including ferrocenoyl–dipeptides,[19] dicobalt hexacarbonyl tagged to alkyne-modified enkephalin,[16] [Mn(Cp)(CO)$_3$] tagged to the cell-penetrating peptides sC18 or hCT(18–32)-k7,[12,15,20] Rh(Cp*)-sandwich,[7] gold(I)[21] or platinum(IV) bioconjugates of TAT, pseudoneurotensin or octreotate.[8,22]

Surprisingly, only little is known about bioconjugates of anticancer half-sandwich ruthenium(II) and osmium(II) organometallics with peptide carriers[9,23] or pendant amino acids.[24,25] This is probably related to synthetic difficulties arising from hydrolysis of the metal–halido bond in aqueous solution, which is a crucial activation parameter for these

[a] Dr. S. M. Meier, M. Novak, Dr. W. Kandioller, Dr. M. A. Jakupec, Prof. Dr. V. B. Arion, Prof. Dr. B. K. Keppler, Prof. Dr. C. G. Hartinger
Institute of Inorganic Chemistry, University of Vienna
Waehringer Strasse 42, 1090 Vienna (Austria)

[b] Dr. S. M. Meier, Dr. W. Kandioller, Dr. M. A. Jakupec, Prof. Dr. B. K. Keppler, Prof. Dr. C. G. Hartinger
Research Platform "Translational Cancer Therapy Research"
University of Vienna, Waehringer Strasse 42, 1090 Vienna (Austria)

[c] Prof. Dr. N. Metzler-Nolte
Inorganic Chemistry I–Bioinorganic Chemistry
Faculty of Chemistry and Biochemistry, Ruhr-University Bochum
Universitätsstrasse 150, 48801 Bochum (Germany)

[d] Prof. Dr. C. G. Hartinger
School of Chemical Sciences, University of Auckland
Private Bag 92019, Auckland 1142 (New Zealand)
E-mail: c.hartinger@auckland.ac.nz

Supporting information for this article is available on the WWW under http://dx.doi.org/10.1002/chem.201300889.

classes of anticancer metallodrugs in a biological setting.[26] The few existing investigations show that loading of the metallodrug on a peptide carrier is associated with a decrease in antiproliferative activity compared to the non-conjugated small metallodrug.[9,23] In particular, conjugation of an Os(arene) picolinate moiety to an octaarginine sequence led to a substantial activity decrease and moderate cytotoxicity was only obtained in protein depleted fetal calf serum.[9] Moreover, conjugation of an imidazole-modified dicarba analogue of octreotide to a Ru(arene)(triphenylphosphine) moiety also resulted in modest cytotoxic activity, which was approximately fourfold lower than that of the analogous small anticancer metallodrug.[23]

The apparent lack of anticancer active organometallic Ru–peptide conjugates from potent metallodrugs prompted us to investigate an appropriate model system with the aim of identifying its cytotoxicity-determining building block(s). The neuropeptide [Leu^5]-enkephalin was chosen for this purpose, and an N-terminal alkyne derivative thereof was further modified by a copper(I)-assisted alkyne–azide cyclization (CuAAC) using 2-(azidomethyl)-5-hydroxy-4*H*-pyran-4-one as a linker to the organometallic moiety. Hydroxypyrones are well-known metal chelators offering *O*,*O*-bidentate coordination,[27] and recent developments involving hydroxypyrones as ligands for organometallic Ru- and Os(arene) compounds with anticancer properties showed intriguing results with respect to in vitro antitumor activity.[28–34] For example, dinuclear ruthenium bis-pyridonato complexes display cytotoxic activity in cell culture assays in dependence of the spacer length separating the two Ru-chelating pyridone moieties. In contrast, several mononuclear organometallic Ru compounds based on *O*,*O*-bidentate pyrones were found to exhibit anticancer activity only in the high micromolar range whereas a substantial increase in activity was observed with *S*,*O*-bidentate thiopyrones, which have been less investigated so far.[31,32,34–36] Based on the mentioned components, that is, Ru(arene), hydroxypyrone, triazole linker and peptide, we aimed to elucidate the structural determinants for anticancer activity of this bioconjugate in human tumor cells.

accumulation in a certain (cancer) tissue or even a specific cell compartment, and they are being studied as promising vectors in the discovery and design of metal-based anticancer agents with targeting properties.[2,14] Most often, the cytotoxic moiety is conjugated to the peptide using an inert linker with the aim of generating a cytotoxic metal–peptide bioconjugate. In the case of organometallic Ru- and Os(arene) compounds, conjugation to peptides often results in a significant reduction of the antiproliferative activity of the metal–peptide bioconjugate compared to the small molecule metallodrug.[8,9] Therefore, it was aimed to investigate a Ru(arene)-based bioconjugate exhibiting antiproliferative activity in vitro and to identify the cytotoxicity-determining building block by comparing the antiproliferative activity of the bioconjugate with lower molecular weight fragments of related structural components.

The linker for the conjugation of the Ru(arene) fragment to the peptide, that is, 2-(azidomethyl)-5-hydroxy-4*H*-pyran-4-one (**1**), was obtained in two steps starting from kojic acid by adapting a published procedure.[37] Compound **1** contains two functional moieties of interest: the pyrone scaffold permits anionic *O*,*O*-bidentate metal coordination, and the azide allows facile and selective modification of the ligand. Importantly, the azide was modified in a single step by CuAAC (Scheme 1).[38–40]

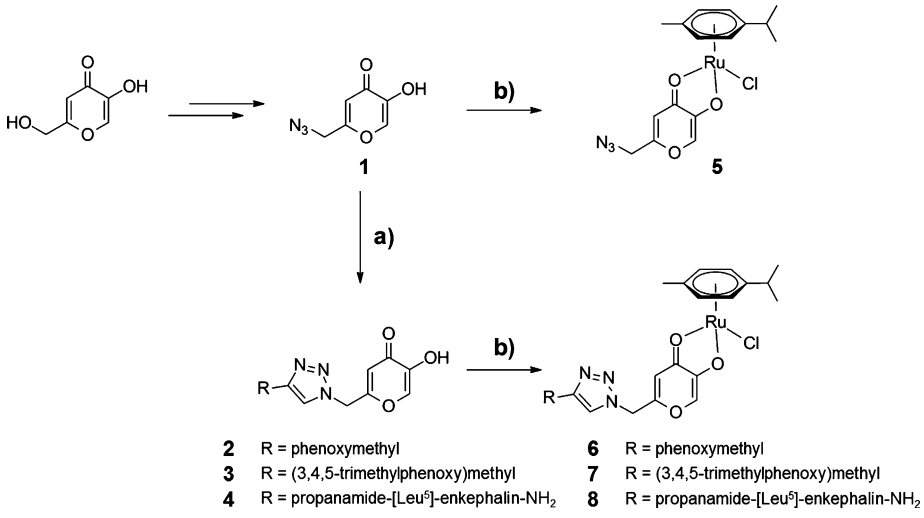

Scheme 1. Synthetic pathway to neutral pyronato complexes, starting from kojic acid. a) This step features CuAAC. b) The complexation step involves deprotonation of the hydroxypyrone prior to coordination leading to neutral [Ru(η^6-*p*-cymene)(Pyr)Cl] complexes, where Pyr is the pyronato ligand.

Results and Discussion

Synthesis and characterization: Peptide carrier systems are an attractive means for obtaining specificity with respect to

The cycloaddition involves the reaction of an azide and a terminal alkyne and allows the introduction of a metal chelator in virtually any molecule containing a terminal alkyne. Copper(I) catalysis yields regioselectively 1,4-substituted triazoles by transient formation of a Cu–acetylide species and represents a powerful tool for extending SARs of the pyronato class of metallodrugs. In metal-based anticancer research, the 1,2,3-triazole pharmacophore is not yet well-established in the therapeutic context, although its

value in diagnostics is well appreciated.[11,41] Copper(I) was prepared in situ from $CuSO_4$ and sodium ascorbate, and the cycloaddition reaction products **2** and **3** were isolated in moderate yields. The molecular structure of **2** was obtained by single crystal X-ray diffraction analysis confirming the formation of the 1,4-substituted triazole (Figure S1 in the Supporting Information). The alkyne-modified [Leu^5]-enkephalin was prepared adapting a literature procedure.[16] The cycloaddition reaction with **1** was carried out on solid support, thus, a suspension of the Rink amide resin was treated with 2 equiv Cu^I and an excess of nitrogen base. Diethyldithiocarbamate (Cupral) proved to be suitable for efficiently removing Cu from the suspension after the reaction. The desired hydroxypyrone-modified [Leu^5]-enkephalin **4** was obtained in 58% overall yield after cleavage from the Rink amide resin.

Complexation of the hydroxypyrones to the Ru(cym) moiety was achieved by deprotonation of the ligand and subsequent addition of 0.5 equiv bis[dichlorido(η^6-*p*-cymene)ruthenium(II)] in dry methanol under an inert atmosphere, similarly to earlier studies.[33] Salt impurities were removed by dissolving the reaction product in DCM, followed by filtration. In general, subsequent precipitation yielded analytically pure products of **5**, **6** and **7** in moderate to high yields (63–82%). The peptide conjugate **8** was treated similarly, since an attempt of performing the cycloaddition reaction with **5** and the alkyne-modified [Leu^5]-enkephalin on solid support had been unsuccessful, probably due to the harsh conditions used during work-up and the pyronato organometallics being known to be acid labile.[34] Complexes **5**, **6** and **7** were characterized by 1D/2D NMR spectroscopy, UHR ESI-TOF MS and elemental analysis. The peptide conjugate **8** was characterized by 1D/2D NMR spectroscopy, UHR ESI-TOF MS and HPLC-MS (see Figure S3 in the Supporting Information for the analytical HPLC-MS experiment).

The modification at the azide moiety is directly detectable in the ^{1}H NMR spectrum (recorded in [D$_6$]DMSO), by comparing in particular the H-7 (CH_2) signals (see Figure 1 and Figure S1 in the Supporting Information for the NMR numbering scheme). The H-7 signal of **1** displays a singlet with a chemical shift of 4.42 ppm. Conversion of the azide into a 1,4-substituted triazole is characterized by a down-field shift of the H-7 singlet (CH_2) to 5.61 ppm. The detection of an additional singlet at approximately 8.3 ppm in **6**, **7** and **8** is indicative of H-8 (H_{Triaz}), the proton in the 1,4-substituted triazole ring. Upon complexation, the ^{1}H NMR signals corresponding to H-7 and H-8 did not shift significantly. However, the H-6 signal underwent an up-field shift by approximately 0.2 ppm. This indicates that the pyronato moiety but not the triazole nitrogen is involved in coordination to the metal, corresponding to a pendant design of triazole complexes, in contrast to the "click-to-chelate" strategy, where the triazole is directly involved in metal-binding.[11,42] *O*,*O*,*N*-Chelation is sterically improbable as can be deduced from Figure 1 and Figure S1 in the Supporting Information. Finally, the chemical shifts of the coordinated cym and pyrone moieties are generally in good agreement with those of the close analogue [chlorido(η^6-*p*-cymene)(2-hydroxymethyl-5-oxo-4*H*-pyronato)ruthenium(II)].[33]

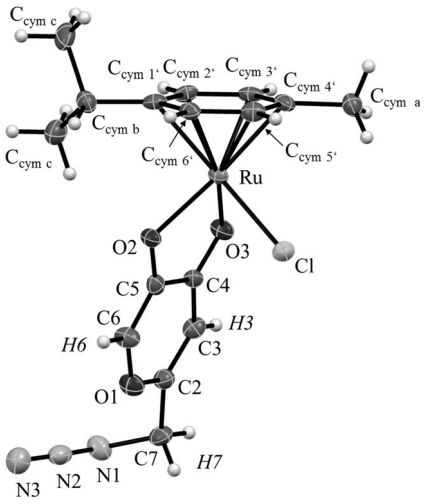

Figure 1. The molecular structure of an enantiomer of **5** is shown including the general numbering scheme. The ellipsoids are drawn at 50% probability level.

X-ray diffraction analysis: Single crystals of **5** suitable for X-ray diffraction analysis were obtained by slow diffusion of *n*-pentane into a dichloromethane solution of the compound. The result of the X-ray diffraction study is shown in Figure 1. Details of data collection, structure solution and refinement, as well as geometrical parameters of **5** are listed in the Supporting Information (Tables S1 and S2). The complex displays the characteristic half-sandwich "piano-stool" configuration. The crystal structure confirms anionic *O*,*O*-bidentate chelation of the pyronato moiety to the metal center yielding a neutral monochlorido complex (Figure 1). Crystal cell parameters and selected bond lengths, angles and torsion angles are listed in the Supporting Information (Tables S1 and S2). Interestingly, both enantiomers were observed at a 1:1 ratio in the crystal of **5**. The asymmetric unit of **5** additionally contains two stereo-isoforms, which feature varying bond lengths in the first coordination sphere (Figure S2 in the Supporting Information). The isoform **5B** shows shorter Ru–O3 and Ru–Cl bond lengths, but longer Ru–O2 and Ru–centroid bond lengths compared to **5A**. In general, the bond lengths and angles are on the same order as observed for related Ru–pyronato and –pyridonato complexes.[29,33] It is noteworthy, that the azide does not degrade during the complexation reaction.

Top-down ESI-MS characterization of the half-sandwich ruthenium peptide bioconjugate: In addition to NMR spectroscopy, analytical HPLC and UHR ESI-TOF MS analysis, the peptide bioconjugate **8** was characterized by tandem mass spectrometric methods in a top-down approach using both ESI-IT and UHR ESI-TOF MS. In principle, top-down MS allows the determination of the sequence of amino acids

and of the site of pyrone modification and metal coordination.

Investigations were performed using collision-induced dissociation (CID) and electron transfer dissociation (ETD, only for IT), which often deliver complementary information due to underlying differences in the fragmentation mechanisms.[43,44] In general, ESI-IT- and ESI-TOF-MS of **8** yield singly and doubly charged species corresponding to $\mathbf{8}_{\mathbf{hydr}}$, $[\mathbf{8}_{\mathbf{hydr}}+H]^{2+}$ and $[\mathbf{8}_{\mathbf{hydr}}+Na]^{2+}$ (all experimental and theoretical signals are listed in Table S3 in the Supporting Information). The notation $\mathbf{8}_{\mathbf{hydr}}$ describes the mass signal corresponding to $[\mathbf{8}-Cl]^{+}$.

ETD relies on the transfer of electrons from a radical anion to the analyte and leads to specific fragmentations of the peptide backbone.[44] ETD of the doubly charged ion $[\mathbf{8}_{\mathbf{hydr}}+H]^{2+}$ yields primarily three species; a charge-reduced species $[\mathbf{8}_{\mathbf{hydr}}+H]^{+}$, a $[(cym)Ru(C_6H_4O_3)]^{\bullet+}$ radical cation and the most abundant mass signal corresponding to $[\mathbf{8}_{\mathbf{hydr}}-(cym)]^{+}$. Therefore, it seems that ETD fragmentation leads primarily to arene cleavage, probably induced by a one-electron reduction of the metal during the electron transfer process (Figure S4 in the Supporting Information). This result was underlined by additional CID investigation of the isolated charge-reduced species (CRCID)[45] corresponding to $[\mathbf{8}_{\mathbf{hydr}}-(cym)]^{+}$. The most abundant signal in the MS mass spectrum corresponds to $[\mathbf{8}_{\mathbf{hydr}}-(cym)-GGFL]^{+}$. This species was found at *m/z* 512.02 suggesting a ruthenium(I) species, since ruthenium(II) would have led to the detection of a signal at *m/z* 511.02. The mass signal of $[Ru(cym)(C_6H_4O_3)]^{\bullet+}$ in the ETD spectrum proves that the pyrone-modified [Leu^5]-enkephalin coordinates via the pyronato moiety to the metal center, however, no information on the peptide sequence was obtained.

On the other hand, CID of the $\mathbf{8}_{\mathbf{hydr}}$ parent signal with 75 eV yielded a more detailed fragmentation picture (Figure 2). The IT and TOF instruments yielded similar fragmentation patterns in the CID spectra, but a higher fragmentation efficiency was observed on the IT instrument. In fact, complete sequence coverage was obtained confirming the amino acid sequence of the modified [Leu^5]-enkephalin. CID leads to strand breaks of the peptide backbone at the amide CO–N bond, which generates predominately positively charged acylium ions corresponding to b-fragments and the complementary amine y-fragments.[43] In the context of metallated peptides, capital letters are used to denote metallated peptide fragments.[46] The occurrence of a complete set of B-fragments indicates that the charged metal must be near the N terminus, where [Leu^5]-enkephalin was modified with the pyrone. Again, the radical β-fragment corresponding to $[Ru(cym)(C_6H_4O_3)]^{\bullet+}$ (*m/z* 360.0292, $m_{ex}=360.0298$, 2 ppm) underlines that the metal–peptide conjugate is formed via metal coordination to the pyronato moiety. Additional secondary fragmentation products (A-fragments) were observed, which were assigned to aldimine ions.

Stability in aqueous solution: Aqueous stability of metallodrugs destined for clinical applications is a crucial prerequisite for drug development. In addition, when considering the class of (thio)pyr(id)onato metallodrugs the ability to resist ligand cleavage from the metal was determined as a second key parameter for obtaining cytotoxic compounds.[31,47] Therefore, the stability of the organometallic complexes **5**, **6** and the bioconjugate **8** was investigated in aqueous solution by ESI-IT mass spectrometry over a period of 48 h. The stability of **7** was not determined because the solubility in aqueous solution is insufficient for performing cytotoxicity assays. Compounds **5** and **8** proved to be stable over the entire incubation period. For each compound the characteristic $\mathbf{M}_{\mathbf{hydr}}$ mass signal was detected corresponding to $[\mathbf{M}-Cl]^{+}$, where $\mathbf{M}=\mathbf{5}$, **6**, **8**. An additional signal at *m/z* 373.94 ± 0.02 ($m_{ex}=374.03$, $<5\,\%$) was detected in the mass spectrum of **5**, which can be assigned to a species formed through loss of N_2 from the azide during the

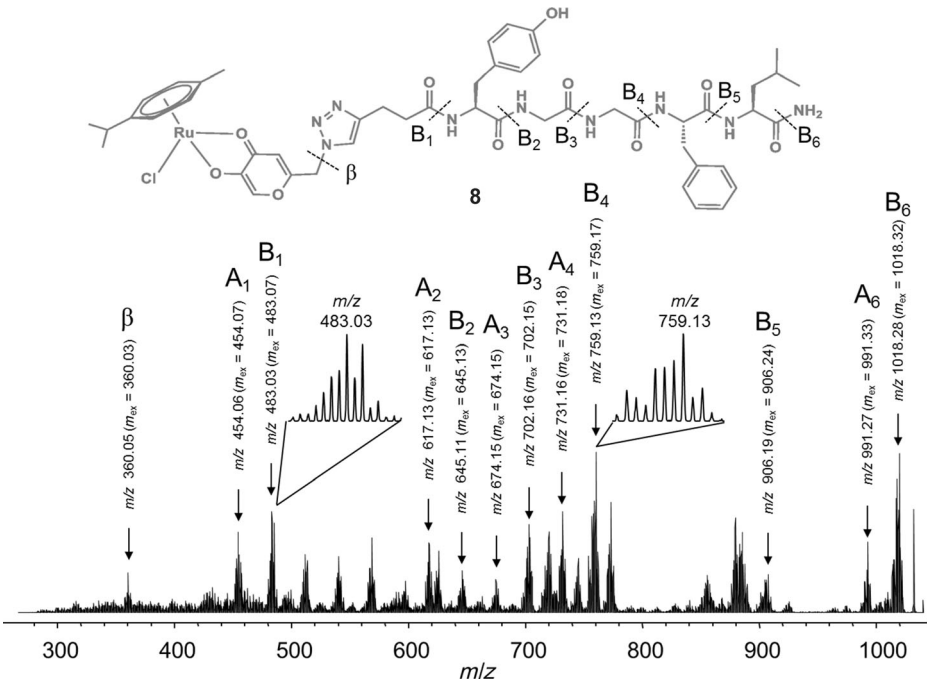

Figure 2. CID tandem mass spectrum of $\mathbf{8}_{\mathbf{hydr}}$ measured on an ESI-IT MS using a collision energy of 75 eV. The identified fragments were labeled according to classical peptide fragment nomenclature; β denotes the radical cation, whereas capital letters denote metallated fragments.

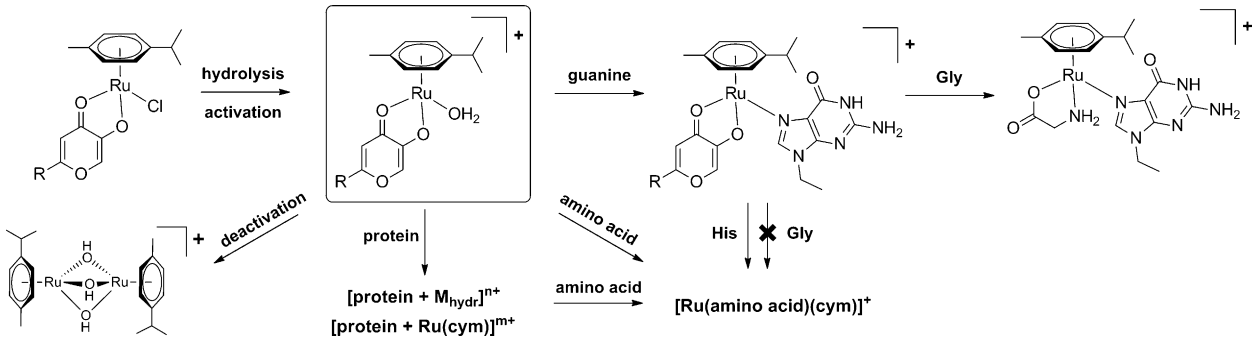

Figure 3. The investigated metabolic pathways of pyronato complexes are illustrated. Organometallic Ru pyronato complexes have to be considered as anticancer prodrugs, which are activated by hydrolysis. For details regarding the stability of the [ub+Ru(cym)]$^{+}$ adduct in the presence of amino acids and other biological nucleophiles, see ref. [47].

spraying process. Compound **6** turned out to be somewhat less stable in aqueous solution. After 24 h, ligand cleavage led to the formation of the dinuclear species $[Ru_2(cym)_2(\mu\text{-}OCH_3)_3]^+$ (6%), which increased to 15% relative to the $\mathbf{6}_{hydr}$ mass signal after 48 h (Figure 3 and Figure S5 in the Supporting Information). The μ-methoxide probably stems from the sample preparation, which involved dilution with H_2O/MeOH (1:1). Aliquots of the same incubation solutions were additionally measured on the MaXis UHR ESI-TOF, and the identities of the $\mathbf{M}_{hydr}$ complexes were confirmed with an accuracy of ≤5 ppm as listed in the Experimental Section.

Table 1. IC_{50} (50% inhibitory concentration) values in three human cancer cell lines after 96 h.

Compound	IC_{50} [μM]		
	CH1	SW480	A549
Ru-kojic acid[a]	234±21	429±10	n.d.[b]
1	264±2	>640	>640
2	194±11	>640	>640
4	>640	>640	>640
5	168±35	224±24	520±46
6	7.6±2.7	170±32	159±52
8	13±5	>320	>320

[a] Taken from ref. [33]; [b] not determined.

In vitro anticancer activity: Organometallic Ru(arene) anticancer agents containing bidentate (thio)pyronato ligands exhibit an intriguing anticancer activity profile. The in vitro cytotoxicity of these metallodrugs as expressed by the IC_{50} value covers a wide range from inactive to active representatives. The anticancer activity of these compounds depends specifically on the ligand choice, and notably hydroxypyrone derivatives are generally noncytotoxic.[32,33,36] Altering the inner coordination sphere form *O*,*O*- to *S*,*O*-chelates leads to a dramatic activity increase and IC_{50} values in the low μM range.[33] Furthermore, the stability of the complexes in the presence of biomolecules appears to be the second parameter determining anticancer activity.[31,47] When peptide carrier systems are employed, organometallic Ru and also Os conjugation often results in a decrease of the antiproliferative activity compared to the structurally related small molecule metallodrugs.[8,9] In the present study, the antiproliferative activity was evaluated in ovarian (CH1), colon (SW480) and non-small lung (A549) cancer cell lines by means of the colorimetric MTT assay.

The bioconjugate precursor **4** is anticancer inactive in vitro, as are the ligands **1** and **2** and the hydrolysis product of the Ru(cym) moiety, that is, $[Ru_2(cym)_2(\mu\text{-}OH)_3]^+$.[31,34] In contrast, the bioconjugate **8** displayed high antiproliferative activity and an IC_{50} value of 13(±5) μM was determined in chemosensitive CH1 cells (Table 1). This represents, to the best of our knowledge, the first example of a half-sandwich Ru bioconjugate with antiproliferative activity in the low μM range. The selective activity in the CH1 cell line parallels the findings with previously reported pyronato complexes.[31–33] It must be noted that pyronato metallodrugs display modest anticancer activity in vitro, whereas the cytotoxicity of the pyronato-based bioconjugate **8** is of the same order of magnitude as that of *S*,*O*-bidentate thiopyronato complexes.[31,33] Roughly comparable to the cytotoxicity of **8** in CH1 cells is that of the bioconjugate model **6**, displaying an IC_{50} value of 7.6(±2.7) μM. On the other hand, compound **5** featuring the free azide is hardly active in vitro, while **7** was found to be too poorly soluble in aqueous media for performing cytotoxicity assays. In our approach, triazole formation in a pendant design seems to be an important parameter with respect to antiproliferative activity of the Ru bioconjugate based on noncytotoxic pyrones. In fact, the antiproliferative activity seems to be independent of the peptide carrier, as **6** and **8** show similar anticancer activities in vitro. Consequently, it is suggested that Ru(cym) in combination with the triazolyl-pyronato linker represents the anticancer-determining building block, which is also supported by the fact that **4** and **5** are inactive in vitro. In principle, this might offer a promising bioconjugation strategy to other cell-penetrating peptides with potential retention of the biological activity.

Reactivity toward biomolecules: Encouraged by the promising results obtained in the in vitro assay, the interaction of the bioconjugate **8** and the model complexes **5** and **6** with

small biomolecules and proteins was studied. Since metallodrugs would usually be administered intravenously, they may react with a broad range of biomolecules in the blood stream, in particular plasma proteins, before reaching the drug target. In order to estimate the reactivity of **5**, **6** and **8** toward biological nucleophiles, they were incubated with the amino acids glycine (Gly), L-cysteine (Cys) and L-histidine (His) and the DNA model 9-ethylguanine (EtG) as well as the proteins ubiquitin (ub) and cytochrome c (cyt). Mass spectrometry has emerged as a powerful technique for the analysis of the interactions between metallodrugs and biomolecules, both with respect to the nature of binding as well as location of binding sites.[46–52] Herein, the experiments were performed with ESI-ion trap (IT) and UHR ESI-time-of-flight (TOF) mass spectrometry. ESI-IT MS was employed for analyzing small molecules, whereas high resolution ESI-TOF MS was used for protein interaction studies.

Similar to **5** and **6**, the reactions of the bioconjugate **8** with amino acids are characterized by ligand cleavage from the metal and formation of $[Ru(aa)(cym)]^+$ (aa = amino acid) adducts similarly to related Ru-pyr(id)onato metallodrugs (Figure 3).[29,47] Such a behavior was observed in the presence of Cys and His, but also to some extent in the presence of Gly (Figure S6 and Table S3 in the Supporting Information). Cys turned out to be the most potent amino acid and induced quantitative ligand cleavage, which may be related to the *trans* effect of the thiol group. Initially, several Cys adducts were detected in the mass spectra, which convert after 48 h, however, to the thermodynamically most stable adduct corresponding to $[Ru(cym)(Cys)]^+$. His with its imidazole side chain was also able to form metal adducts through ligand cleavage, although the kinetics of this reaction were slightly slower than for Cys. His leads to quantitative depletion of the signals assignable to $\mathbf{5}_{hydr}$, $\mathbf{6}_{hydr}$ and $\mathbf{8}_{hydr}$ in the mass spectra within 6 h. The conjugate model $\mathbf{6}_{hydr}$ was slightly more resistant to ligand cleavage, which was reflected in a lower percentage of $[Ru(cym)(His)]^+$ adduct formation (68%) compared to $\mathbf{5}_{hydr}$ and $\mathbf{8}_{hydr}$ (>85%) after 1 h. In contrast to previous reports, the reaction with Gly was also characterized by adduct formation and ligand cleavage from the metal, albeit to a low extent. Interestingly, mono- and bis-adducts were formed during the reaction corresponding to $[Ru(cym)(Gly)]^+$ and $[Ru(cym)(Gly)_2]^+$. The occurrence of bis-adducts is probably related to the reduced steric demand of the amino acid. However, Gly was not able to completely consume the free complexes over an incubation period of 48 h (Figure S6 in the Supporting Information). Binding of Gly was least pronounced for the bioconjugate **8** possibly due to steric reasons.

Furthermore, the reaction with EtG, used as a DNA model, resulted in the formation of $[\mathbf{M}_{hydr}+EtG]^+$ adducts ($\mathbf{M}$ = **5**, **6** and **8**) possibly via N7 of guanine and was characterized by ligand retention, which can be explained by the monodentate character of the interaction. Despite the increased molar ratio (2:1 EtG/Ru), EtG adducts did not exceed a relative abundance of 36% (relative to $\mathbf{M}_{hydr}$) and only monoadducts were observed within 48 h. EtG adduct formation seems to depend again on the steric demand of the ligand, with **5** forming 36% of adducts after 48 h and the bioconjugate **8** forming only 6% adducts with EtG. The following trend for the reactivity toward EtG was observed: **5** > **6** > **8**. The stability of the $[\mathbf{6}_{hydr}+EtG]^+$ adduct in the presence of His and Gly was additionally investigated (Figure S7 in the Supporting Information). For this purpose, **6** was incubated with EtG for 5 days prior to the addition of 2 equiv of either Gly or His. Addition of His led to quantitative conversion of $\mathbf{6}_{hydr}$ and $[\mathbf{6}_{hydr}+EtG]^+$ to the $[Ru(cym)(His)]^+$ adduct within 3 h. Addition of Gly did not entirely deplete the $[\mathbf{6}_{hydr}+EtG]^+$ adduct within 24 h. However, Gly seems to react with $\mathbf{6}_{hydr}$ forming a mixed ligand adduct with free EtG corresponding to $[Ru(cym)(EtG)(Gly)]^+$, which becomes the most abundant species after 24 h. The absence of an analogous adduct upon addition of His indicates a possible tridentate binding mode of His to the metal.

The subtle differences in reactivity of the bioconjugate **8** (and its cytotoxic model **6**) on the one hand and **5** on the other hand with small biomolecules suggest that slower kinetics of adduct formation and ligand cleavage from the metal are associated with increased in vitro cytotoxic activity, which is also in accordance with an earlier study on pyronato metallodrugs.[47]

Moreover, it seems that the compounds in this study interact preferentially with amino acids rather than with nucleobases, suggesting that Ru metallodrugs containing the pyronato scaffold probably have a cellular target different from DNA and more likely related to proteins (Figure 3). Consequently, **5**, **6** and **8** were additionally analyzed with respect to their reactivity toward the proteins ubiquitin (ub) and cytochrome c (cyt) by using UHR ESI-TOF mass spectrometry.

Binding to ub was found to be accompanied by ligand cleavage from the metal, giving rise to the characteristic $[ub+Ru(cym)]^+$ adducts when incubating ub with the bioconjugate **8** or its models **5** or **6** (Table S3 in the Supporting Information). Ubiquitin features two probable binding partners for a Ru ion, namely the N-terminal methionine (Met1) and histidine at position 68 (His68). It was suggested that Met1 may act as a bidentate binding partner to a metallodrug,[50,53] which may increase reaction kinetics and also adduct stability. Mono-adducts are most probably formed by metallation of Met1, as recently determined in a top-down ESI-MS analysis of the $[ub+Ru(cym)]^+$ adduct.[54] The ESI-TOF MS experiments yielded detailed information on the adduct types, that is, bis-adducts corresponding to $[ub+2Ru(cym)]^+$ were also detected in small amounts indicating metallation of His68 to a minor degree. Interestingly, bis-adducts with ub were detected only at 1 and 6% relative abundance for **8** and **6**, respectively, whereas they were present at 12% relative abundance for **5**.

The incubation with cyt at a molar ratio of 3:1 was characterized by two types of mono-adducts. Similar to the experiments with ub, the most abundant adduct corresponds to $[cyt+Ru(cym)]^+$. Despite the addition of a molar excess of the metallodrug, bis-adducts were not observed. Addi-

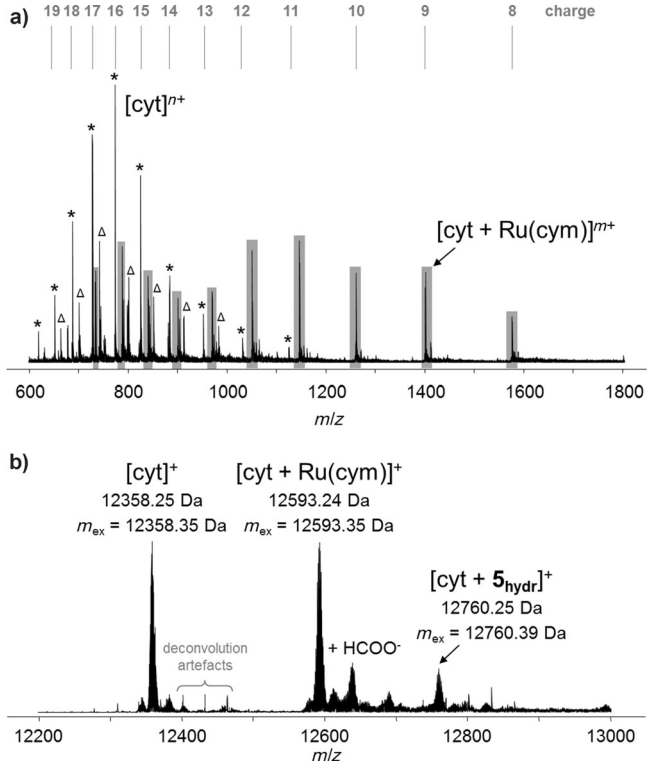

Figure 4. a) Charge state distributions observed in the broadband ESI-TOF mass spectrum of the incubation mixture containing **5** and cyt at a 3:1 metal-to-protein ratio. Free cyt is detected at high charge states (*) indicating complete loss of the tertiary structure, similar to [cyt+$\mathbf{5}_{hydr}$]$^+$ (Δ), which can only bind in a monodentate coordination mode. On the other hand, the lower charge state distribution of the [cyt+Ru(cym)]$^+$ adduct (grey) indicates the cross-linking ability of the Ru(cym) moiety. The spectrum was recorded under denaturing conditions. b) The deconvoluted UHR ESI-TOF mass spectrum of the same experiment is shown. A cyt adduct with intact $\mathbf{5}_{hydr}$ was detected at 12760.25 Da.

tional [cyt+$\mathbf{M}_{hydr}$]$^+$ adducts were observed in all three cases and were characterized by ligand retention, for example, [cyt+$\mathbf{5}_{hydr}$]$^+$ (13%, Figure 4b). After 48 h, the relative abundance of the combined mono-adducts formed with the bioconjugate **8** and the model **6** corresponds to 41(±4)%, compared to 64% for the inactive model **5**.

The kinetics of adduct formation are significantly lower for cyt than for ub, which is attributed to the presence of different binding partners in these proteins. Cytochrome c contains three accessible metal binding sites, His26, His33 and Met65, that are mono-dentate binding partners similar to His68 in ub. It is, therefore, assumed that the ability of bidentate Met1 binding in ub is responsible for the kinetic differences of adduct formation observed for ub and cyt. Furthermore, the lack of potential bidentate binding partners in cyt may be responsible for the observation of stable $\mathbf{M}_{hydr}$–cyt adducts. Again, the slightly slower kinetics of adduct formation with proteins for **6** and **8** compared to **5** are reflected in their increased antiproliferative activity in vitro.

When comparing the charge state distributions of free cyt and the mono-adduct under denaturing conditions (50% MeOH, 0.2% formic acid) in the broadband ESI-TOF mass spectrum, most of the charge states for free cyt are found between +12 and +19 referring to entirely denatured protein (labeled with *, Figure 4a).[55] The adduct [cyt+$\mathbf{5}_{hydr}$]$^+$ displays roughly the same charge distribution, indicating that mono-dentate binding of the organometallic fragment to the protein does not influence its tertiary structure (labeled with Δ, Figure 4a). Interestingly, the [cyt+Ru(cym)]$^+$ adduct shows two charge state populations, with the first population showing charge states of +13 to +17 indicative of a completely unfolded protein (Figure 4a, grey) similar to free cyt. In contrast, the second population with charge states from +8 to +13 refers to a partially folded protein and suggests a cross-linking of the protein backbone by the Ru(cym) fragment. The first population may correspond to Ru(cym) binding to His26 and/or His33, which does not affect the protein tertiary structure. On the other hand, the second population may correspond to Ru(cym) binding to His33 and Met65, leading to the observed cross-linking effect in MS experiments. This behavior was observed exclusively for **5**, **6** and **8** incubated with cyt but not with ub. This is an intriguing aspect, since the function of proteins highly depends on their tertiary structure and consequently, protein cross-linking might play a role in the mode of action of the investigated metallodrugs.

Conclusion

Attaching a cytotoxic moiety to peptide carrier systems has attracted much interest, for example, because this opens up new possibilities for drug targeting with cell-penetrating peptides. However, conjugation of organometallic Ru and also Os anticancer agents to a peptide carrier usually resulted in a reduction of the antiproliferative activity compared to the small metallodrug alone. Here, a metal bioconjugation strategy is pursued in which the opposite effect was observed, and to the best of our knowledge, the first organometallic half-sandwich Ru bioconjugate displaying antiproliferative activity in the low micromolar range (in CH1 ovarian cancer cells) is reported, whereas the non-metallated peptide **4** is completely inactive. The comparison of the Ru bioconjugate **8** with the smaller bioconjugate models **5** and **6**, which can be considered building blocks of **8**, revealed that the anticancer potency seems to be independent of the peptide carrier, whereas the triazole moiety is essential, suggesting the Ru(cym) species with the triazolyl-pyronato linker as the minimal structural requirement for activity in vitro. The identification of this cytotoxic moiety may open an approach to a wider range of anticancer active Ru bioconjugates. High resolution top-down ESI-MS was performed confirming the expected amino acid sequence, linker modification and metallation site in **8** and providing a useful approach for characterizing organometal–peptide bioconjugates. Finally, ESI-MS studies provided insights into their molecular reactivity toward biomolecules and proteins, and a delayed reactivity of the bioconjugate toward the biomole-

cules seems to be reflected in an increased in vitro cytotoxicity.

Experimental Section

Materials and methods: All reactions were carried out in dry solvents and under inert atmosphere. Chemicals obtained from commercial suppliers were used as received and were of analytical grade. Methanol and dichloromethane were dried using standard procedures. $RuCl_3 \cdot 3H_2O$ (40.4%) was purchased from Johnson Matthey; ubiquitin (bovine erythrocytes), horse heart cytochrome c, dimethyl sulfoxide (DMSO) and 9-ethylguanine from Sigma; *N,N*-dimethylformamide (extra dry), 2-propanol, propargylbromide (80%, stabilized in toluene), α-terpinene and tetrahydrofuran from Acros; copper(II) sulfate pentahydrate, phenol and 3,4,5-trimethylphenol from Fisher; L-histidine and potassium carbonate from Merck; L-methionine, sodium ascorbate, sodium azide, sodium methoxide, thionyl chloride and triphenylphosphite from Sigma–Aldrich and kojic acid from TCI Europe. Methanol (VWR Int., HiPerSolv CHROMANORM), formic acid (Fluka) and MilliQ H_2O (18.2 MΩ, Advantage A10, 185 UV Ultrapure Water System, Millipore, France) were used in ESI-MS studies. The dimer bis[dichlorido(η^6-*p*-cymene)ruthenium(II)][56,57] and the ligand 2-(azidomethyl)-5-hydroxy-4*H*-pyran-4-one[37] were synthesized as previously described.

NMR spectra were recorded at 25 °C on a Bruker FT NMR spectrometer Avance III™ 500 MHz at 500.10 (^{1}H), 202.63 MHz (^{31}P{^{1}H}) and 125.75 MHz (^{13}C{^{1}H}) and 2D NMR data were collected in a gradient-enhanced mode. Hydrogen and carbon atoms were numbered according to crystal structure numbering. Elemental analysis was carried out on a Perkin–Elmer 2400 CHN elemental analyzer by the Laboratory for Elemental Analysis, Faculty of Chemistry, University of Vienna. An analytical HPLC system (TM100, Dionex) was equipped with a reversed-phased column (Zorbax Eclipse Plus C18, Agilent, 5 μm pore size, 4.6 μm inner diameter and 250 mm column length), that was thermostated at 25 °C, and a UV-detector (UVD 170U, Dionex). The flow rate was 1 mL min^{-1} using a H_2O/MeOH (95:5) eluent ratio for the first 3 min. Afterwards, a linear gradient was employed starting with H_2O/MeOH (95:5) and ending with H_2O/MeOH (5:95) for 15 min, which was then kept for 5 min. TFA (0.1%) was added to all eluents. The HPLC was coupled to an AmaZon ESI-ion trap mass spectrometer (Bruker Daltonics GmbH, Bremen, Germany) and controlled by Chromeleon 6.8 software (Thermo Scientific, Bremen, Germany). Electrospray ionization mass spectra were recorded on a Bruker AmaZon SL, a Bruker AmaZon Speed ETD ion trap (IT) and on a UHR MaXis time-of-flight (TOF) mass spectrometer (Bruker Daltonics GmbH, Bremen, Germany). Collision-induced dissociation (CID) was performed using 50–75 eV collision energy, whereas 100–300 ms reaction times were employed for electron transfer dissociation (ETD) experiments on the AmaZon Speed ETD. Data were acquired and processed using Compass 1.3 and Data Analysis 4.0 (Bruker Daltonics GmbH, Bremen, Germany). Deconvolution was obtained by applying the maximum entropy algorithm with a 0.1 *m/z* mass step and 0.5 *m/z* instrument peak width for the IT and automatic data point spacing and 30000 instrument resolving power for the TOF. X-ray diffraction measurements of single crystals were performed on a Bruker X8 APEX II CCD diffractometer at 100 K. CCDC-902337 (**2**), and 902338 (**5**) contain the supplementary crystallographic data for this paper. These data can be obtained free of charge from The Cambridge Crystallographic Data Centre via www.ccdc.cam.ac.uk/data_request/cif. The single crystals of **2** and **5** were positioned at 35 mm from the detector. A total of 1141 frames for 60 s over 1° were measured for **2** and 2039 frames for 20 s over 1° for **5**. The data were processed using the SAINT Plus software package.[58] Crystal data, data collection parameters, and structure refinement details are given in Table S1 in the Supporting Information. The structure was solved by direct methods and refined by full-matrix least-squares techniques. Non-hydrogen atoms were refined with anisotropic displacement parameters. H atoms were inserted at calculated positions and refined with a riding model. The following software programs and tables were used: structure solution SHELXS-97,[59] refinement SHELXL-97,[59] molecular diagrams Mercury CSD 3.0.[60]

Interaction with biomolecules: Samples for ESI-MS were analyzed by direct infusion at a flow rate of 3 μL min^{-1} and at typical concentrations of 1–5 μM. Protein samples were analyzed under denaturing conditions by diluting them with water/methanol/formic acid (50:50:0.2), whereas the reference complexes and small molecule samples were diluted with water/methanol (50:50). Stock solutions of compound **5** and **8** were prepared in H_2O, whereas **6** was dissolved in aqueous solution containing 1% DSMO. The following molar ratios were used for interaction studies at 37 °C and pH 5.5: ub/**M** (1:2), cyt/**M** (1:3), amino acid/**M** (1:1) and EtG/**M** (2:1), where **M** is the respective Ru metallodrug. Mass spectra were recorded after 1, 3, 6, 24 and 48 h. In general, relative intensities correspond to percentages of the area under peaks of the sum of all assignable metal signals in the spectrum.

Cell lines and culture conditions: CH1 cells (ovarian adenocarcinoma, human) were provided by Lloyd R. Kelland (CRC Centre for Cancer Therapeutics, Institute of Cancer Research, Sutton, UK), SW480 (adenocarcinoma of the colon, human) and A549 (non-small cell lung cancer, human) cells were provided by Brigitte Marian (Institute of Cancer Research, Department of Medicine I, Medical University of Vienna, Austria). All cell culture reagents were purchased from Sigma–Aldrich. Cells were grown in 75 cm^2 culture flasks (Starlab) as adherent monolayer cultures in Eagle's minimal essential medium (MEM) supplemented with heat-inactivated fetal calf serum (10%), sodium pyruvate (1 mM), L-glutamine (4 mM) and non-essential amino acids (1% v/v; from 100× ready-to-use stock). Cultures were maintained at 37 °C in a humidified atmosphere containing 95% air and 5% CO_2.

Cytotoxicity in cancer cell lines: Cytotoxicity was determined by the colorimetric MTT (3-(4,5-dimethyl-2-thiazolyl)-2,5-diphenyl-2*H*-tetrazolium bromide; Sigma–Aldrich) microculture assay. For this purpose, cells were harvested from culture flasks by trypsinization and seeded in aliquots (100 μL) of complete MEM (see above) into 96-well microculture plates (Starlab). Cell densities of 1.0×10^3 cells per well (CH1), 2.0×10^3 cells per well (SW480) and 3.0×10^3 cells per well (A549) were chosen in order to ensure exponential growth of untreated controls throughout the experiment. Cells were allowed to settle and resume exponential growth for 24 h. Compound **1** was dissolved directly in complete MEM, whereas all other test compounds were dissolved in DMSO first and then serially diluted in complete MEM such that the effective DMSO content did not exceed 0.5% (v/v). Dilutions were added in aliquots (100 μL) to the microcultures, and cells were exposed to the test compounds for 96 h. At the end of the exposure period, all media were replaced with 100 μL per well of a 6:1 mixture of RPMI1640 medium (supplemented with 10% heat-inactivated fetal calf serum and 2 mM L-glutamine) and MTT solution (5 mg mL^{-1} phosphate-buffered saline). After incubation for 4 h, the supernatants were removed, and the formazan product formed by viable cells was dissolved in 150 μL DMSO per well. Optical densities at 550 nm were measured with a microplate reader (BioTek ELx808), by using a reference wavelength of 690 nm to correct for unspecific absorption. The quantity of viable cells was expressed in terms of T/C values by comparison to untreated control microcultures, and 50% inhibitory concentrations (IC_{50}) were calculated from concentration-effect curves by interpolation. Evaluation is based on means from at least three independent experiments, each comprising three replicates per concentration level.

Synthesis

(Prop-2-yn-1-yloxy)benzene: Phenol (3.00 g, 32 mmol) and propargyl bromide (3.56 mL, 32 mmol) were added in a 100 mL round flask containing dry DMF (30 mL) and potassium carbonate (6.62 g, 48 mmol). The reaction mixture was stirred for 18 h under argon atmosphere at room temperature. The product was extracted with dichloromethane (3×50 mL), the combined extracts were washed with H_2O (50 mL) and dried over anhydrous Na_2SO_4. The solution was concentrated yielding the crude product as a yellow oil, which was purified by flash-column chromatography using *n*-hexane/dichloromethane as eluent (1:1.1). Yield: 2.20 g (52%); ^{1}H NMR (500.10 MHz, [D$_6$]DMSO): $\delta = 7.31$ (dd, ^3J(H,H) = 7 Hz, ^3J(H,H) = 7 Hz, 2H, $H_{Ar3',5'}$), 6.99–6.94 (m, 3H, $H_{Ar2',4',6'}$), 4.78 (d, ^4J(H,H) = 2 Hz, 2H, $-CH_2$), 3.55 ppm (t, ^4J(H,H) = 2 Hz, 1H, $-C\equiv CH$);

$^{13}C\{^1H\}$ NMR (125.75 MHz, [D$_6$]DMSO): $\delta = 157.1$ ($C_{Ar1'}$), 129.4 ($C_{Ar2',6'}$), 121.09 ($C_{Ar4'}$), 114.7 ($C_{Ar3',5'}$), 78.0 (−C≡*C*H), 55.2 ppm (−*C*H$_2$).

1,2,3-Trimethyl-5-(prop-2-yn-1-yloxy)benzene: In a 100 mL round flask, 3,4,5-trimethylphenol (1.36 g, 10 mmol) was dissolved in acetone (50 mL). Propargyl bromide (0.90 mL, 11 mmol) and potassium carbonate (1.52 g, 11 mmol) were added. The reaction mixture was refluxed at 65 °C for 24 h. Water (20 mL) was added and the pH adjusted to 12 with NaOH. The product was quickly extracted with dichloromethane (3× 20 mL). The combined organic phase was dried over anhydrous Na_2SO_4 and subsequently filtered. The solvent was removed yielding the product as a yellow oil. Yield: 1.61 g (89 %); ^1H NMR (500.10 MHz, [D$_6$]DMSO): $\delta = 6.62$ (s, 2H, H_{Ar}), 4.69 (d, ^4J(H,H) = 3 Hz, 2H, −C*H*$_2$), 3.49 (t, ^4J(H,H) = 3 Hz, 1H, −C≡C*H*), 2.20 (s, 6H, $C_{Ar3',5'}$ −C*H*$_3$), 2.03 ppm (s, 3H, $C_{Ar4'}$ −C*H*$_3$); $^{13}C\{^1H\}$ NMR (125.75 MHz, [D$_6$]DMSO): $\delta = 154.3$ ($C_{Ar1'}$), 136.9 ($C_{Ar3',5'}$), 126.7 ($C_{Ar4'}$), 113.8 ($C_{Ar2',6'}$), 77.7 (−*C*≡CH), 55.1 (−*C*H$_2$), 20.4 ($C_{Ar3',5'}$ −*C*H$_3$), 14.2 ppm ($C_{Ar4'}$ −*C*H$_3$); MS (ESI$^+$): *m/z* 175.13 $[M+H]^+$ ($m_{ex} = 175.11$).

*2-(Azidomethyl)-5-hydroxy-4H-pyran-4-one (**1**)*: The procedure of Atkinson et al. was used with minor modifications.[37] Step 1: thionyl chloride (19.5 mL, 271 mmol) was added to kojic acid (7.00 g, 50 mmol) under vigorous stirring at 0 °C. After complete addition, the reaction was stirred for 4 h and the remaining thionyl chloride was removed under reduced pressure using a cooling trap. The dry yellowish reaction product was suspended in *n*-hexane and filtered. Recrystallization from *i*PrOH yielded colorless crystals of 2-(chloromethyl)-5-hydroxy-pyran-4*H*-one, which were dried in vacuo. Yield: 6.60 g (84 %); ^1H NMR (500.10 MHz, [D$_6$]DMSO): $\delta = 9.29$ (s, 1H, −O*H*), 8.12 (s, 1H, H-6), 6.56 (s, 1H, H-3), 4.66 ppm (s, 2H, H-7). Step 2: in a round-bottom flask, sodium azide (1.22 g, 19 mmol) was suspended in dry DMF (12.3 mL) under argon atmosphere at 0 °C. Then 2-(chloromethyl)-5-hydroxy-pyran-4*H*-one (3.00 g, 19 mmol) was slowly added and the reaction mixture became turbid after several minutes. The suspension was allowed to warm to room temperature and was stirred in the absence of light for 24 h, before it was slowly poured into H_2O (7.5 mL, 0 °C). A colorless solid precipitated, which was separated by filtration and dried in vacuo. Yield: 2.71 g (87 %); ^1H NMR (500.10 MHz, [D$_6$]DMSO): $\delta = 9.24$ (s, 1H, −O*H*), 8.11 (s, 1H, H-6), 6.45 (s, 1H, H-3), 4.42 ppm (s, 2H, H-7); $^{13}C\{^1H\}$ NMR (125.75 MHz, [D$_6$]DMSO, 25 °C): $\delta = 174.1$ (C-4), 162.3 (C-2), 146.4 (C-5), 140.5 (C-6), 113.0 (C-3), 50.6 ppm (C-7); elemental analysis calcd for $C_6H_5N_3O_3$: C 43.12, H 3.02, N 25.14; found: C 43.11, H 2.76, N 24.97; MS (ESI$^+$): *m/z* 168.11 $[M+H]^+$ ($m_{ex} = 168.04$).

*5-Hydroxy-2-{(4-(phenoxymethyl)-1H-1,2,3-triazol-1-yl)methyl}-4H-pyran-4-one (**2**)*: Copper sulfate pentahydrate (30 mg, 10 mol %) and sodium ascorbate (95.1 mg, 40 mol %) were suspended in deoxygenated H_2O (2.5 mL) and stirred until the reaction mixture turned yellow. This reaction mixture was added to a suspension of **1** (200 mg, 1.2 mmol) and (prop-2-yn-1-yloxy)benzene (237 mg, 1.8 mmol) in deoxygenated argon-flushed H_2O/THF (7.5 mL, 1:2). The reaction mixture was stirred for 24 h at room temperature under argon atmosphere and then the solvent was removed. The residue was dissolved in ethyl acetate, dried over anhydrous Na_2SO_4 and filtered. After removal of the solvent and recrystallization from *i*PrOH, the yellowish product was obtained after filtration and dried in vacuo. Yield: 165 mg (46 %); ^1H NMR (500.10 MHz, [D$_6$]DMSO): $\delta = 9.28$ (s, 1H, −O*H*), 8.33 (s, 1H, H-8), 8.06 (s, 1H, H-6), 7.30 (t, ^3J(H,H) = 8 Hz, 2H, $H_{Ar3',5'}$), 7.03 (d, ^3J(H,H) = 8 Hz, 2H, $H_{Ar2',6'}$), 6.95 (t, ^3J(H,H) = 8 Hz, 1H, $H_{Ar4'}$), 6.40 (s, 1H, H-3), 5.61 (s, 2H, H-7), 5.16 ppm (s, 2H, H-10); $^{13}C\{^1H\}$ NMR (125.75 MHz, [D$_6$]DMSO): $\delta =$ 173.5 (C-4), 160.5 (C-2), 157.9 ($C_{Ar1'}$), 145.9 (C-5), 143.1 (C-9), 139.9 (C-6), 129.4 ($C_{Ar3',5'}$), 125.3 (C-8), 120.8 ($C_{Ar4'}$), 114.6 ($C_{Ar2',6'}$), 113.0 (C-3), 60.8 (C-10), 49.9 ppm (C-7); elemental analysis calcd for $C_{15}H_{13}N_3O_4 \cdot 0.4\,H_2O$: C 58.78, H 4.54, N 13.71; found: C 59.05, H 4.14, N 13.32; MS (ESI$^-$): *m/z* 298.15 $[M-H]^-$ ($m_{ex} = 298.08$).

*5-Hydroxy-2-{(4-[(3,4,5-trimethylphenoxy)methyl]-1H-1,2,3-triazol-1-yl)-methyl}-4H-pyran-4-one (**3**)*: Copper sulfate pentahydrate (30 mg, 10 mol %) and sodium ascorbate (95 mg, 40 mol %) were suspended in deoxygenated H_2O (2.5 mL) and stirred until the mixture turned yellow. This reaction mixture was then added to the suspension of **1** (200 mg, 1.2 mmol) and 1,2,3-trimethyl-5-(prop-2-yn-1-yloxy)benzene (314 mg, 1.8 mmol) in deoxygenated, argon-flushed H_2O/THF (7.5 mL, 1:2). The reaction mixture was stirred for 24 h at room temperature after which the solvent was evaporated. The residue was dissolved in ethyl acetate, dried over anhydrous Na_2SO_4 and filtered. After removal of the solvent and recrystallization from *i*PrOH, the yellowish product was obtained after filtration and dried in vacuo. Yield: 260 mg (64 %); ^1H NMR (500.10 MHz, [D$_6$]DMSO): $\delta = 9.28$ (s, 1H, −O*H*), 8.29 (s, 1H, H-8), 8.05 (s, 1H, H-6), 6.67 (s, 2H, $H_{Ar2',6'}$), 6.38 (s, 1H, H-3), 5.60 (s, 2H, H-7), 5.08 (s, 2H, H-10), 2.19 (s, 6H, $C_{Ar3',5'}$ −C*H*$_3$), 2.03 ppm (s, 3H, $C_{Ar4'}$ −C*H*$_3$); $^{13}C\{^1H\}$ NMR (125.75 MHz, [D$_6$]DMSO): $\delta = 173.5$ (C-4), 160.5 (C-2), 155.2 ($C_{Ar1'}$), 145.9 (C-5), 143.4 (C-9), 139.9 (C-6), 136.9 ($C_{Ar3',5'}$), 126.7 ($C_{Ar4'}$), 125.1 (C-8), 113.7 ($C_{Ar2',6'}$), 112.9 (C-3), 60.7 (C-10), 49.8 (C-7), 20.3 ($C_{Ar4'}$ −CH$_3$), 14.2 ppm ($C_{Ar3',5'}$ −*C*H$_3$); MS (ESI$^+$): *m/z* 342.10 $[M+H]^+$ ($m_{ex} = 342.15$).

*5-Hydroxy-2-{((4-(N-tyrosinyl-glycinyl-glycinyl-phenylallanyl-leucinyl-NH$_2$)propanamido)-1H-1,2,3-triazol-1-yl)methyl}-4H-pyran-4-one (**4**)*: The Fmoc-protected [Leu^5]-enkephalin was manually prepared on Rink amide resins (500 mg, 0.36 mmol) according to standard solid-phase synthesis procedures[16,61] using a fourfold excess of the Fmoc-protected amino acid. Each coupling was performed in the presence of TBTU (433 mg, 1.35 mmol), HOBT (192 mg, 1.35 mmol) and DIPEA (618 μL, 0.36 mmol) and 4-pentynoic acid was coupled in the same manner. The solid-phase CuAAC was performed adapting a procedure by Tornoe et al.[39] and Koester et al.[62] Compound **1** (119 mg, 0.71 mmol) was dissolved in ACN/DCM (2:1, 6 mL) and purged with N_2. CuI (135 mg, 0.71 mmol) was dissolved in ACN/DCM (2:1, 8 mL) and both compounds were transferred into the syringe containing the resin (500 mg, 0.36 mmol). Finally, DIPEA (2.98 mL, 18 mmol, 50 equiv) was taken up in the syringe and the mixture was shaken at room temperature in the absence of light for 18 h under N_2. After washing with DMF (5×4 mL, 2 min), Cu impurities were removed with a 0.14 M solution of cupral (0.71 mmol) in DMF and again washed with DMF (5×4 mL, 2 min) and DCM (5×4 mL, 2 min). The modified peptide was cleaved from the resin by treatment with 7 mL of TFA/TIS/H_2O (95:2.5:2.5) for 2 h and then precipitated by addition of cold diethyl ether. After centrifugation, the solution was decanted and the product was washed twice with cold diethyl ether and finally dried in vacuo. After purification by preparative HPLC and lyophilization, the product was obtained as a colourless solid. Yield: 166 mg (58 %); ^1H NMR (500.10 MHz, [D$_6$]DMSO): $\delta = 9.18$ (br s, 1H, −OH$_{Tyr}$), 8.26 (t, ^3J(H,H) = 6 Hz, 1H, −NH$_{Gly}$), 8.14 (d, ^3J(H,H) = 8 Hz, 1H, −NH$_{Leu}$), 8.06 (d, ^3J(H,H) = 8 Hz, 1H, −NH$_{Tyr}$), 8.03 (s, 1H, H-8), 7.99 (t, ^3J(H,H) = 6 Hz, 1H, −NH$_{Phe}$), 7.96 (d, ^3J(H,H) = 8 Hz, 1H, −NH$_{Gly}$), 7.81 (s, 1H, H-6), 7.24 (d, ^3J(H,H) = 5 Hz, 4H, $H_{Ar,Phe}$), 7.17–7.14 (m, 1H, $H_{Ar,Phe}$), 7.09 (s, 1H, −NH$_2$), 7.00 (d, ^3J(H,H) = 9 Hz, 2, $H_{Ar,Tyr}$), 6.97 (s, 1H, −NH$_2$), 6.62 (d, ^3J(H,H) = 9 Hz, 2, $H_{Ar,Tyr}$), 6.36 (s, 1H, H-3), 5.49 (s, 2H, H-7), 4.53–4.48 (m, 1H, $H_{\alpha,Phe}$), 4.42–4.39 (m, 1H, $H_{\alpha,Tyr}$), 4.22–4.17 (m, 1H, $H_{\alpha,Leu}$), 3.72–3.69 (m, 4H, $H_{\alpha,Gly}$), 3.03 (dd, ^2J(H,H) = 14 Hz, ^3J(H,H) = 5 Hz, 2H, $H_{\beta,Tyr}$), 2.92 (dd, ^2J(H,H) = 14 Hz, ^3J(H,H) = 5 Hz, 2H, $H_{\beta,Phe}$), 2.76 (t, ^3J(H,H) = 9 Hz, 2H, $H_{\alpha,pent}$), 2.64 (t, ^3J(H,H) = 9 Hz, 2H, $H_{\beta,pent}$), 1.60–1.52 (m, 1H, $H_{\gamma,Leu}$), 1.48–1.45 (m, 2H, $H_{\beta,Leu}$), 0.84 ppm (dd, ^2J(H,H) = 26 Hz, ^3J(H,H) = 7 Hz, 6H, $H_{\delta,Leu}$); MS (ESI$^+$): *m/z* 802.23 $[M+H]^+$ ($m_{ex} = 802.35$), MS (ESI$^-$): *m/z* 914.44 $[M-H+TFA]^-$ ($m_{ex} = 914.33$); anal. HPLC: 11.26 min.

General procedure for the synthesis of [chlorido(η^6-p-cymene)-(pyronato)ruthenium(II)] complexes: The pyrone ligand (1–1.1 equiv) and sodium methoxide (1–1.1 equiv) were suspended in dry methanol under argon atmosphere at room temperature and stirred for 15 min. Then bis-[dichlorido(η^6-*p*-cymene)ruthenium(II)] (0.5 equiv) was added and the clear, orange-red colored solution was stirred for further 6–18 h. The solvent was removed under reduced pressure, the residue was dissolved in dichloromethane, filtered and the filtrate was concentrated to a final volume of about 2–3 mL. The product was precipitated by addition of *n*-hexane, filtered and dried in vacuo.

*[{2-(Azidomethyl)-5-oxo-κO-4H-pyronato-κO}chlorido(η^6-p-cymene)ruthenium(II)] (**5**)*: The reaction was performed according to the general procedure using pyrone **1** (40 mg, 0.23 mmol), sodium methoxide (13 mg, 0.23 mmol), bis[dichlorido(η^6-*p*-cymene)ruthenium(II)] (70 mg, 0.16 mmol) and methanol (8 mL). The product was isolated as brownish

crystals. Reaction time: 18 h. Yield: 65 mg (65%); ^{1}H NMR (500.10 MHz, [D$_6$]DMSO): δ = 7.93 (s, 1H, H-6), 6.68 (s, 1H, H-3), 5.70–5.68 (m, 2H, H$_{Cym3',5'}$), 5.42–5.40 (m, 2H, H$_{Cym2',6'}$), 4.43 (s, 2H, H-7), 2.76 (sept, ^3J(H,H) = 7 Hz, 1H, H$_{Cymb}$), 2.14 (s, 3H, H$_{Cyma}$), 1.25 ppm (dd, ^3J(H,H) = 7 Hz, ^4J(H,H) = 2 Hz, 6H, H$_{Cymc}$); ^{13}C{^{1}H} NMR (125.75 MHz, [D$_6$]DMSO): δ = 185.2 (C-4), 161.5 (C-2), 159.9 (C-5), 140.8 (C-6), 108.8 (C-3), 97.9 (C$_{Cym1'}$), 94.9 (C$_{Cym4'}$), 79.9 (C$_{Cym3',5'}$), 76.9 (C$_{Cym2',6'}$), 49.8 (C-7), 30.5 (C$_{Cymb}$), 22.0 (C$_{Cymc}$), 17.9 ppm (C$_{Cyma}$); elemental analysis calcd for C$_{16}$H$_{18}$ClN$_3$O$_3$Ru·$^1/_3$H$_2$O: C 43.39, H 4.25, N 9.48; found: C 43.79, H 3.97, N 9.09; MS (ESI$^+$): *m/z* 402.0377 [*M*−Cl]$^+$ (m_{ex} = 402.0391, 4 ppm), 374.0311 [*M*−Cl−N$_2$]$^+$ (m_{ex} = 374.0329, 5 ppm).

*[Chlorido(η^6-p-cymene){5-oxo-κO-2-([(4-(phenoxymethyl)-1H-1,2,3-triazol-1-yl]methyl)-4H-pyronato-κO}ruthenium(II)] (**6**)*: The reaction was performed according to the general procedure using pyrone **2** (100 mg, 0.33 mmol), sodium methoxide (18 mg, 0.34 mmol), bis[dichlorido(η^6-*p*-cymene)ruthenium(II)] (99 mg, 0.16 mmol) and methanol (10 mL). The product was isolated as yellow microcrystals. Reaction time: 18 h. Yield: 115 mg (63%); ^{1}H NMR (500.10 MHz, [D$_6$]DMSO): δ = 8.30 (s, 1H, H-8), 7.87 (s, 1H, H-6), 7.30 (t, ^3J(H,H) = 8 Hz, 2H, H$_{Ar3',5'}$), 7.02 (d, ^3J(H,H) = 8 Hz, 2H, H$_{Ar2',6'}$), 6.95 (t, ^3J(H,H) = 8 Hz, 1H, H$_{Ar4'}$), 6.61 (s, 1H, H-3), 5.69–5.67 (m, 2H, H$_{Cym3',5'}$), 5.62 (s, 2H, H-7), 5.41–5.39 (m, 2H, H$_{Cym2',6'}$), 5.14 (s, 2H, H-10), 2.76 (sept, ^3J(H,H) = 7 Hz, 1H, H$_{Cymb}$), 2.13 (s, 3H, H$_{Cyma}$), 1.25 ppm (d, ^3J(H,H) = 7 Hz, 6H, H$_{Cymc}$); ^{13}C{^{1}H} NMR (125.75 MHz, [D$_6$]DMSO, 25 °C): δ = 185.2 (C-4), 160.1 (C-2), 160.0 (C-5), 157.9 (C$_{Ar1'}$), 143.2 (C-9), 140.8 (C-6), 129.4 (C$_{Ar3',5'}$), 126.0 (C-8), 120.8 (C$_{Ar4'}$), 114.6 (C$_{Ar2',6'}$), 109.1 (C-3), 97.9 (C$_{Cym1'}$), 94.9 (C$_{Cym4'}$), 79.9 (C$_{Cym3',5'}$), 77.0 (C$_{Cym2',6'}$), 60.7 (C-10), 49.6 (C-7), 30.6 (C$_{Cymb}$), 22.0 (C$_{Cymc}$), 17.9 ppm (C$_{Cyma}$); elemental analysis calcd for C$_{25}$H$_{26}$ClN$_3$O$_4$Ru·0.5H$_2$O: C 51.95, H 4.71, N 7.27; found: C 52.14, H 4.36, N 7.30; MS (ESI$^+$): *m/z* 534.0947 [*M*−Cl]$^+$ (m_{ex} = 534.0968, 4 ppm).

*[Chlorido(η^6-p-cymene){5-oxo-κO-2-[(4-((3,4,5-trimethylphenoxy)methyl)-1H-1,2,3-triazol-1-yl)methyl]-4H-pyronato-κO}ruthenium(II)] (**7**)*: The reaction was performed according to the general procedure using pyrone **3** (112 mg, 0.33 mmol), sodium methoxide (18 mg, 0.34 mmol), bis[dichlorido(η^6-*p*-cymene)ruthenium(II)] (99 mg, 0.16 mmol) and methanol (10 mL). The product was isolated as yellow solid. Reaction time: 18 h. Yield: 160 mg (82%); ^{1}H NMR (500.10 MHz, [D$_6$]DMSO): δ = 8.26 (s, 1H, H-8), 7.88 (s, 1H, H-6), 6.67 (s, 2H, H$_{Ar2',6'}$), 6.59 (s, 1H, H-3), 5.69–5.67 (m, 2H, H$_{Cym3',5'}$), 5.61 (s, 2H, H-7), 5.41–5.39 (m, 2H, H$_{Cym2',6'}$), 5.06 (s, 2H, H-10), 2.76 (sept, ^3J(H,H) = 7 Hz, 1H, H$_{Cymb}$), 2.19 (s, 6H, C$_{Ar3',5'}$−CH$_3$), 2.13 (s, 3H, H$_{Cyma}$), 2.03 (s, 3H, C$_{Ar4'}$−CH$_3$), 1.25 ppm (d, ^3J(H,H) = 7 Hz, 6H, H$_{Cymc}$); ^{13}C{^{1}H} NMR (125.75 MHz, [D$_6$]DMSO): δ = 185.2 (C-4), 160.2 (C-2), 160.0 (C-5), 155.2 (C$_{Ar1'}$), 143.4 (C-9), 140.8 (C-6), 136.9 (C$_{Ar3',5'}$), 126.7 (C$_{Ar4'}$), 126.0 (C-8), 113.6 (C$_{Ar2',6'}$), 109.0 (C-3), 97.9 (C$_{Cym1'}$), 94.9 (C$_{Cym4'}$), 79.9 (C$_{Cym3',5'}$), 77.0 (C$_{Cym2',6'}$), 60.7 (C-10), 49.6 (C-7), 30.6 (C$_{Cymb}$), 22.0 (C$_{Cymc}$), 20.3 (C$_{Ar3',5'}$ −CH$_3$), 17.9 (C$_{Cyma}$), 14.2 ppm (C$_{Ar4'}$ −CH$_3$); elemental analysis calcd for C$_{28}$H$_{32}$ClN$_3$O$_4$Ru·0.5H$_2$O: C 54.23, H 5.36, N 6.78; found: C 53.98, H 4.97, N 6.81; MS (ESI$^+$): *m/z* 576.1406 [*M*−Cl]$^+$ (m_{ex} = 576.1433, 5 ppm).

*[Chlorido(η^6-p-cymene)(5-oxo-κO-2-[(4-[(N-tyrosinyl-glycinyl-glycinyl-phenylallanyl-leucinyl-NH$_2$)propanamido]-1H-1,2,3-triazol-1-yl)methyl]-4H-pyronato-κO)ruthenium(II)] (**8**)*: The reaction was performed according to the general procedure using pyrone **4** (18.3 mg, 0.02 mmol), sodium methoxide (2.2 mg, 0.04 mmol), bis[dichlorido(η^6-*p*-cymene)ruthenium(II)] (6.4 mg, 0.01 mmol) and methanol (4 mL). The reaction was stirred for 6 h in the absence of light at room temperature and under an inert atmosphere. A yellow solution was obtained, which was concentrated and the residue was dried in vacuo. Preparative HPLC and subsequent lyophilization yielded the desired product as a yellow powder. Yield: 11.7 mg (51%); ^{1}H NMR (500.10 MHz, [D$_6$]DMSO): δ = 9.15 (s, 1H, −OH$_{Tyr}$), 8.24 (t, ^3J(H,H) = 7 Hz, 1H, −NH$_{Gly}$), 8.24 (s, 1H, H-8), 8.12 (d, ^3J(H,H) = 8 Hz, 1H, −NH$_{Leu}$), 8.06 (d, ^3J(H,H) = 8 Hz, 1H, −NH$_{Tyr}$), 7.99 (d, ^3J(H,H) = 6 Hz, 1H, −NH$_{Phe}$), 7.95 (t, ^3J(H,H) = 7 Hz, 1H, −NH$_{Gly}$), 7.80 (s, 1H, H-6), 7.24 (d, ^3J(H,H) = 5 Hz, 4H, H$_{Ar,Phe}$), 7.19–7.15 (m, 1H, H$_{Ar,Phe}$), 7.09 (brs, 1H, −NH$_2$), 7.00 (d, ^3J(H,H) = 9 Hz, 2H, H$_{Ar,Tyr}$), 6.96 (brs, 1H, −NH$_2$), 6.62 (d, ^3J(H,H) = 9 Hz, 2H, H$_{Ar,Tyr}$), 6.35 (s, 1H, H-3), 5.69–5.66 (m, 2H, H$_{Cym3',5'}$), 5.59 (s, 2H, H-7), 5.41–5.39 (m, 2H, H$_{Cym2',6'}$), 4.51–4.49 (m, 1H, H$_{\alpha,Phe}$), 4.44–4.40 (m, 1H, H$_{\alpha,Tyr}$), 4.20 (q, ^3J(H,H) = 7.5 Hz, H$_{\alpha,Leu}$), 3.73–3.62 (m, 4H, H$_{\alpha,Gly}$), 3.03 (dd, ^2J(H,H) = 14 Hz, ^3J(H,H) = 5 Hz, 1H, H$_{\beta,Tyr}$), 2.92 (dd, ^2J = 14 Hz, ^3J(H,H) = 5 Hz, 2H, H$_{\beta,Phe}$), 2.78–2.74 (m, 2H, H$_{\beta,Pent}$), 2.66–2.61 (m, 2H, H$_{\alpha,Pent}$), 2.16 (s, 3H, H$_{Cyma}$ H-1′), 1.60–1.52 (m, 1H, H$_{\gamma,Leu}$), 1.46 (t, ^3J(H,H) = 7 Hz, 2H, H$_{\beta,Leu}$), 1.27 (d, ^3J(H,H) = 7 Hz, 6H, H$_{Cymc}$), 0.85 ppm (dd, ^3J(H,H) = 25 Hz, ^3J(H,H) = 7 Hz, 6H, H$_{\delta,Leu}$); MS (ESI$^+$): *m/z* 518.6773 [*M*−Cl+H]$^{2+}$ (m_{ex} = 518.6794, 4 ppm); anal. HPLC: 12.2 min.

Acknowledgements

We would like to thank COST D39 and CM1105 and the Johanna Mahlke née Obermann Foundation for financial support, and the Mass Spectrometry Center (Faculty of Chemistry, University of Vienna) for access to the UHR ESI-TOF mass spectrometer. We gratefully acknowledge Alexander Roller for collecting the X-ray diffraction data. S.M.M. thanks in particular S. David Köster, H. Bauke Albada and Kathrin Klein for their support at RUB, and Elisabeth Jirkovsky for several ESI-MS measurements.

[1] N. Yamamoto, N. S. Bryce, N. Metzler-Nolte, T. W. Hambley, *Bioconjugate Chem.* **2012**, *23*, 1110–1118.
[2] F. Milletti, *Drug Discovery Today* **2012**, *17*, 850–860.
[3] C. G. Hartinger, N. Metzler-Nolte, P. J. Dyson, *Organometallics* **2012**, *31*, 5677–5685.
[4] Q. Geng, X. Sun, T. Gong, Z. R. Zhang, *Bioconjugate Chem.* **2012**, *23*, 1200–1210.
[5] K. L. Horton, K. M. Stewart, S. B. Fonseca, Q. Guo, S. O. Kelley, *Chem. Biol.* **2008**, *15*, 375–382.
[6] G. Gasser, N. Metzler-Nolte, *Curr. Opin. Chem. Biol.* **2012**, *16*, 84–91.
[7] H. B. Albada, F. Wieberneit, I. Dijkgraaf, J. H. Harvey, J. L. Whistler, R. Stoll, N. Metzler-Nolte, R. H. Fish, *J. Am. Chem. Soc.* **2012**, *134*, 10321–10324.
[8] S. Abramkin, S. M. Valiahdi, M. A. Jakupec, M. Galanski, N. Metzler-Nolte, B. K. Keppler, *Dalton Trans.* **2012**, *41*, 3001–3005.
[9] S. H. van Rijt, H. Kostrhunova, V. Brabec, P. J. Sadler, *Bioconjugate Chem.* **2011**, *22*, 218–226.
[10] A. Gross, M. Neukamm, N. Metzler-Nolte, *Dalton Trans.* **2011**, *40*, 1382–1386.
[11] H. Struthers, T. L. Mindt, R. Schibli, *Dalton Trans.* **2010**, *39*, 675–696.
[12] K. Splith, W. N. Hu, U. Schatzschneider, R. Gust, I. Ott, L. A. Onambele, A. Prokop, I. Neundorf, *Bioconjugate Chem.* **2010**, *21*, 1288–1296.
[13] A. Pinto, U. Hoffmanns, M. Ott, G. Fricker, N. Metzler-Nolte, *ChemBioChem* **2009**, *10*, 1852–1860.
[14] N. Metzler-Nolte, in *Topics in Organometallic Chemistry Vol. 32* (Eds: G. Jaouen, N. Metzler-Nolte), Springer, Heidelberg, **2009**, pp. 195–217.
[15] I. Neundorf, J. Hoyer, K. Splith, R. Rennert, H. W. P. N′Dongo, U. Schatzschneider, *Chem. Commun.* **2008**, 5604–5606.
[16] M. A. Neukamm, A. Pinto, N. Metzler-Nolte, *Chem. Commun.* **2008**, 232–234.
[17] E. García-Garayoa, R. Schibli, P. A. Schubiger, *Nucl. Sci. Tech.* **2007**, *18*, 88–100.
[18] D. B. Grotjahn, *Coord. Chem. Rev.* **1999**, *190–192*, 1125–1141.
[19] A. Mooney, A. J. Corry, D. O'Sullivan, K. R. Dilip, P. T. M. Kenny, *J. Organomet. Chem.* **2009**, *694*, 886–894.
[20] H. W. P. N′Dongo, I. Ott, R. Gust, U. Schatzschneider, *J. Organomet. Chem.* **2009**, *694*, 823–827.
[21] S. D. Köster, H. Alborzinia, S. Z. Can, I. Kitanovic, S. Wolfl, R. Rubbiani, I. Ott, P. Riesterer, A. Prokop, K. Merz, N. Metzler-Nolte, *Chem. Sci.* **2012**, *3*, 2062–2072.
[22] L. Gaviglio, A. Gross, N. Metzler-Nolte, M. Ravera, *Metallomics* **2012**, *4*, 260–266.

[23] F. Barragán, D. Carrion-Salip, I. Gomez-Pinto, A. Gonzalez-Canto, P. J. Sadler, R. de Llorens, V. Moreno, C. Gonzalez, A. Massaguer, V. Marchan, *Bioconjugate Chem.* **2012**, *23*, 1838–1855.
[24] J. Tauchman, G. Suss-Fink, P. Stepnicka, O. Zava, P. J. Dyson, *J. Organomet. Chem.* **2013**, *723*, 233–238.
[25] J. Tauchman, B. Therrien, G. Suss-Fink, P. Stepnicka, *Organometallics* **2012**, *31*, 3985–3994.
[26] A. M. Pizarro, A. Habtemariam, P. J. Sadler, in *Medicinal Organometallic Chemistry* (Eds: G. Jaouen, N. Metzler-Nolte), Springer, Heidelberg, **2010**, pp. 21–56.
[27] M. A. Santos, *Coord. Chem. Rev.* **2008**, *252*, 1213–1224.
[28] W. Kandioller, A. Kurzwernhart, M. Hanif, S. M. Meier, H. Henke, B. K. Keppler, C. G. Hartinger, *J. Organomet. Chem.* **2011**, *696*, 999–1010.
[29] M. Hanif, H. Henke, S. M. Meier, S. Martic, M. Labib, W. Kandioller, M. A. Jakupec, V. B. Arion, H. B. Kraatz, B. K. Keppler, C. G. Hartinger, *Inorg. Chem.* **2010**, *49*, 7953–7963.
[30] M. G. Mendoza-Ferri, C. G. Hartinger, M. A. Mendoza, M. Groessl, A. E. Egger, R. E. Eichinger, J. B. Mangrum, N. P. Farrell, M. Maruszak, P. J. Bednarski, F. Klein, M. A. Jakupec, A. A. Nazarov, K. Severin, B. K. Keppler, *J. Med. Chem.* **2009**, *52*, 916–925.
[31] W. Kandioller, C. G. Hartinger, A. A. Nazarov, M. L. Kuznetsov, R. O. John, C. Bartel, M. A. Jakupec, V. B. Arion, B. K. Keppler, *Organometallics* **2009**, *28*, 4249–4251.
[32] W. Kandioller, C. G. Hartinger, A. A. Nazarov, J. Kasser, R. John, M. A. Jakupec, V. B. Arion, P. J. Dyson, B. K. Keppler, *J. Organomet. Chem.* **2009**, *694*, 922–929.
[33] W. Kandioller, C. G. Hartinger, A. A. Nazarov, C. Bartel, M. Skocic, M. A. Jakupec, V. B. Arion, B. K. Keppler, *Chem. Eur. J.* **2009**, *15*, 12283–12291.
[34] A. F. A. Peacock, M. Melchart, R. J. Deeth, A. Habtemariam, S. Parsons, P. J. Sadler, *Chem. Eur. J.* **2007**, *13*, 2601–2613.
[35] M. Hanif, P. Schaaf, W. Kandioller, M. Hejl, M. A. Jakupec, A. Roller, B. K. Keppler, C. G. Hartinger, *Aust. J. Chem.* **2010**, *63*, 1521–1528.
[36] J. H. Kasser, W. Kandioller, C. G. Hartinger, A. A. Nazarov, V. B. Arion, P. J. Dyson, B. K. Keppler, *J. Organomet. Chem.* **2010**, *695*, 875–881.
[37] J. G. Atkinson, Y. Girard, J. Rokach, C. S. Rooney, C. S. Mcfarlane, A. Rackham, N. N. Share, *J. Med. Chem.* **1979**, *22*, 99–106.
[38] V. V. Rostovtsev, L. G. Green, V. V. Fokin, K. B. Sharpless, *Angew. Chem.* **2002**, *114*, 2708–2711; *Angew. Chem. Int. Ed.* **2002**, *41*, 2596–2599.
[39] C. W. Tornoe, C. Christensen, M. Meldal, *J. Org. Chem.* **2002**, *67*, 3057–3064.
[40] C. F. C. Lam, A. C. Giddens, N. Chand, V. L. Webb, B. R. Copp, *Tetrahedron* **2012**, *68*, 3187–3194.
[41] S. G. Agalave, S. R. Maujan, V. S. Pore, *Chem. Asian J.* **2011**, *6*, 2696–2718.
[42] H. Struthers, B. Spingler, T. L. Mindt, R. Schibli, *Chem. Eur. J.* **2008**, *14*, 6173–6183.
[43] I. A. Papayannopoulos, *Mass Spectrom. Rev.* **1995**, *14*, 49–73.
[44] L. M. Mikesh, B. Ueberheide, A. Chi, J. J. Coon, J. E. Syka, J. Shabanowitz, D. F. Hunt, *Biochim. Biophys. Acta Proteins Proteomics* **2006**, *1764*, 1811–1822.
[45] H. Ben Hamidane, D. Chiappe, R. Hartmer, A. Vorobyev, M. Moniatte, Y. O. Tsybin, *J. Am. Soc. Mass Spectrom.* **2009**, *20*, 567–575.
[46] S. M. Meier, Y. O. Tsybin, P. J. Dyson, B. K. Keppler, C. G. Hartinger, *Anal. Bioanal. Chem.* **2012**, *402*, 2655–2662.
[47] S. M. Meier, M. Hanif, W. Kandioller, B. K. Keppler, C. G. Hartinger, *J. Inorg. Biochem.* **2012**, *108*, 91–95.
[48] N. Zhang, Y. Du, M. Cui, J. Xing, Z. Liu, S. Liu, *Anal. Chem.* **2012**, *84*, 6206–6212.
[49] J. P. Williams, H. I. A. Phillips, I. Campuzano, P. J. Sadler, *J. Am. Soc. Mass Spectrom.* **2010**, *21*, 1097–1106.
[50] J. P. Williams, J. M. Brown, I. Campuzano, P. J. Sadler, *Chem. Commun.* **2010**, *46*, 5458–5460.
[51] A. Casini, C. Gabbiani, E. Michelucci, G. Pieraccini, G. Moneti, P. J. Dyson, L. Messori, *J. Biol. Inorg. Chem.* **2009**, *14*, 761–770.
[52] A. Casini, A. Guerri, C. Gabbiani, L. Messori, *J. Inorg. Biochem.* **2008**, *102*, 995–1006.
[53] D. Gibson, C. E. Costello, *Eur. Mass Spectrom.* **1999**, *5*, 501–510.
[54] W. Kandioller, E. Balsano, S. M. Meier, U. Jungwirth, S. Goschl, A. Roller, M. A. Jakupec, W. Berger, B. K. Keppler, C. G. Hartinger, *Chem. Commun.* **2013**, *49*, 3348–3350.
[55] L. Konermann, D. J. Douglas, *Biochemistry* **1997**, *36*, 12296–12302.
[56] M. A. Bennett, A. K. Smith, *J. Chem. Soc. Dalton Trans.* **1974**, 233–241.
[57] M. A. Bennett, T. N. Huang, T. W. Matheson, A. K. Smith, *Inorg. Synth.* **1982**, *21*, 74–78.
[58] M. R. Pressprich, J. Chambers, *SAINT+Integration Engine*, *Program for Crystal Structure Integration*, Bruker Analytical X-ray systems, Madison, **2004**.
[59] G. M. Sheldrick, *SHELXL-97*, *Program for Crystal Structure Refinement*, University of Göttingen (Germany), **1997**.
[60] C. F. Macrae, I. J. Bruno, J. A. Chisholm, P. R. Edgington, P. McCabe, E. Pidcock, L. Rodriguez-Monge, R. Taylor, J. van de Streek, P. A. Wood, *J. Appl. Crystallogr.* **2008**, *41*, 466–470.
[61] D. R. van Staveren, N. Metzler-Nolte, *Chem. Commun.* **2002**, 1406–1407.
[62] S. D. Köster, J. Dittrich, G. Gasser, N. Husken, I. C. H. Castaneda, J. L. Jios, C. O. Della Vedova, N. Metzler-Nolte, *Organometallics* **2008**, *27*, 6326–6332.

Received: March 7, 2013
Published online: May 27, 2013

